BLADE TWIST EFFECTS ON ROTOR BEHAVIOUR IN THE VORTEX RING STATE

R. E. Brown*
Department of Aeronautics,
Imperial College of Science, Technology & Medicine,
Prince Consort Road,
London SW7 2BY.

J. G. Leishman†
Dept. of Aerospace Engineering,
Glenn L. Martin Institute of Technology
University of Maryland,
College Park, MD 20742, USA.

S. J. Newman‡
Dept. of Aerospace Engineering,
University of Southampton,
Highfield, Southampton SO17 1BJ.

F. J. Perry§
FJ Perry Rotorcraft Consultant,
Yeovil, Somerset BA20 1NU.

Abstract

Results are shown that give a better understanding of the factors that influence the initiation and subsequent development of the vortex ring state (VRS). It is suggested that the onset of VRS is associated with the collapse of the orderly structure of the rotor wake into a highly disturbed, irregular, aperiodic flow state. An analysis of the stability of the wake is presented to show that the location of the boundary of the VRS is influenced by the detailed structure of the rotor wake prior to its breakdown. Time-accurate calculations of the evolution of the rotor wake in the VRS are then presented to obtain more insight into the flows experienced by the rotor in the VRS. These calculations suggest that the location of the boundary of the VRS, and the depth of the VRS regime, is sensitive to the blade spanwise loading distribution, which is influenced by blade twist. The effects are significant even at low disk loading, but at high thrust where rotor stall may be encountered, rotors with and without significant blade twist show marked, and somewhat counterintuitive, differences in their behaviour under VRS conditions.

Nomenclature

A	Rotor disk area, πR^2, m^2
c	Rotor blade chord, m
C_T	Rotor thrust coefficient, $T/(\rho A\Omega^2 R^2)$
C_Q	Rotor torque coefficient, $Q/(\rho A\Omega^2 R^3)$
k	Vorticity transport parameter
Q	Rotor torque, Nm
r,θ,z	Cylindrical polar coodinates, m, rad., m
$\mathbf{r}$	Position vector of a wake marker, m
R	Rotor radius, m
$\mathbf{S}$	Vorticity source, s^{-2}
t	Time, s
T	Rotor thrust, N
v_h	Hover induced velocity, $T/(2\rho A)$, ms^{-1}
v_i	Induced velocity, ms^{-1}
V_c	Climb (out-of-plane) velocity, ms^{-1}
V_∞	Forward (in-plane) velocity, ms^{-1}
$\mathbf{V}$	Velocity vector, ms^{-1}
x,y,z	Cartesian coordinates, m
α_P	Wake perturbation growth rate, s^{-1}
α'_P	Non-dim. growth rate, $\alpha_P/\left(\Gamma_v/4\pi R^2\right)$
Γ_v	Tip vortex strength (circulation), m^{2}s^{-1}
δC_T	Perturbation to thrust coefficient
ζ	Wake (vortex) age, rad
θ_{tw}	Effective linear blade twist per radius, degrees
λ_h	Non-dim. hover induced velocity, $\sqrt{C_T/2}$
$\overline{\lambda}_i$	Induced velocity, scaled by v_h
$\overline{\mu}_W$	Effective wake transport velocity, scaled by v_h
$\overline{\mu}_x$	Non-dimensional forward speed, V_∞/v_h
$\overline{\mu}_z$	Non-dimensional climbing speed, V_c/v_h
ρ	Air density, kg m^{-3}
σ	Rotor solidity, $N_b c/\pi R$
ψ	Azimuth angle, rad
ω	Wake perturbation wave number
$\boldsymbol{\omega}$	Vorticity vector, s^{-1}
Ω	Rotor angular velocity, rads^{-1}

Abbreviations

BVI	Blade Vortex Interaction
FVM	Free-Vortex Model
TWS	Turbulent Wake State
VRS	Vortex Ring State
VTM	Vorticity Transport Model
WBS	Windmill Brake State

* Lecturer.
† Professor.
‡ Senior Lecturer.
§ Consultant.

Presented at the European Rotorcraft Forum, Bristol, England, September 17–20, 2002.

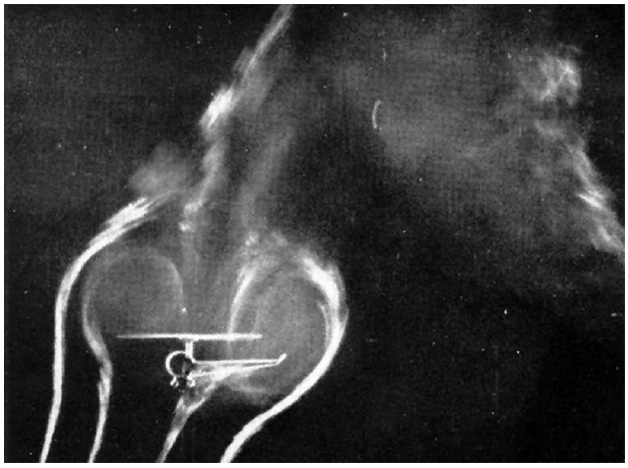

Figure 1: *Smoke flow visualization of a rotor operating in the VRS, showing the characteristic recirculation of the flow in the rotor plane.*

Introduction

While the accurate prediction of rotor flow fields is difficult under most flight conditions, the prediction of the wake dynamics during descending flight has proven to be a particularly challenging problem for the analyst. This is partly because of blade vortex interaction (BVI) and a general susceptibility to unsteadiness and aperiodicity of the rotor wake structure. Under conditions where the upward component of velocity normal to the rotor disk plane is a substantial fraction of the average induced velocity downward through the rotor disk, such as when descending at high rates or steep angles, the rotor can encounter an adverse condition known as the vortex ring state (VRS). Under VRS conditions, the wake vorticity produced by the blades cannot convect away from the rotor and accumulates near the rotor plane, clumping or bundling together and producing large, aperiodic airloads. In aerodynamic terms, the onset of the VRS is associated with the collapse of the orderly structure of the rotor wake into a highly disturbed, irregular, recirculating flow.

A representative example of the complex topology of the flow surrounding a steeply descending helicopter rotor operating in the VRS is shown in Fig. 1, which is taken from the work of Drees & Hendal (Ref. 1). This smoke flow visualization image was taken by illuminating a cross-section through the rotor wake. Deeply into the VRS, the flow near the rotor resembles that of a three-dimensional bluff body operating at low Reynolds numbers, and there is clear evidence of separation and unsteady recirculation of the flow near the rotor.

When a helicopter enters the VRS, it experiences significant rotor thrust fluctuations and an increase in average rotor shaft torque (power required). Power must be applied to overcome the high aerodynamic losses associated with the rotor operating inside its own recirculating wake. Most helicopters have minimal excess power available at low airspeeds, so these losses usually manifest themselves as an uncommanded increase in descent rate. This behaviour of the helicopter is referred to by pilots as "power settling" or "settling with power," and adversely affects flight safety (Ref. 2). The rotor thrust fluctuations in the VRS lead to low-frequency vertical accelerations of the helicopter, and the associated blade flapping can lead to a substantial reduction of control effectiveness and thus to high pilot workload. While operation in the VRS is obviously undesirable, it can be entered inadvertently through poor piloting technique.

Recently, there has been renewed interest in understanding and predicting the flow mechanisms that lead to the onset of the VRS, both for helicopters and for other rotating-wing aircraft such as tiltrotors. For traditional helicopters with low disk loading, the region of the flight envelope affected by the VRS is generally small, and has not overly constrained practical operations. However, it has been suggested (Refs. 3–6) that modern helicopters and tiltrotors, with their very much higher disk loadings, may be susceptible to the VRS over a greater proportion of their low-speed flight envelope. Furthermore, modern military rotorcraft are required to fly a wide range of manoeuvres at low airspeed, including rapid pull-ups, which can increase the upward component of velocity through the disk and may bring the rotor(s) closer to the VRS (Ref. 6). The behaviour of side-by-side configurations, such as tiltrotors, at high rates of descent has come under particular scrutiny because the VRS may be encountered more severely on one rotor compared to the other (Refs. 5–7), possibly requiring large asymmetric loads to be overcome by the aircraft's control system.

The highly nonlinear physics of the VRS is further complicated by the likelihood of flow separation and blade stall on more highly loaded rotors during descending flight. This can occur because of the higher aerodynamic angles of attack produced on the inboard parts of the blades during descent, or, when in the VRS, the blades chop through the accumulations of vorticity engulfing the rotor (Ref. 6). Flight tests (Ref. 8) show that in partial power descent near the VRS the rotor can operate without evidence of blade stall and at relatively low power, but that another state can be reached at the same airspeed and rate of descent where the rotor requires much higher power because of blade stall. This observation suggests that, in addition to the nonlinear behaviour of the wake within the VRS, nonlinearity in the aerodynamics of the blades also plays an important role in governing helicopter behaviour in the VRS.

The results of the present paper confirm that the susceptibility to wake breakdown, and the potential onset of the VRS, depends on several factors that are a consequence of the rotor configuration as well as of its operating state. In particular, it is suggested that, in addition to the disk loading effects mentioned above, the high levels of blade twist inherent in modern helicopter rotor and tiltrotor designs may expand the VRS regime to a wider range of operational descent velocities and to higher forward speeds than is the case for rotors with more lightly-twisted blades. Furthermore, numerical calculations show changes in rotor behaviour, once rotor wake breakdown has occurred, which result from the introduction of high blade twist.

Previous Work

Experimental work is fundamental to understanding the VRS, but instrumented flight tests with helicopters operating in the VRS are sparse, mainly because it is a difficult flight condition in which to sustain equilibrium flight. The flight tests of Scheiman (Ref. 8) revealed the highly unsteady blade loads and high rotor power requirements that characterize flight in the VRS. Other flight tests have revealed that geometrically similar helicopters may exhibit different handling characteristics when flown in the VRS (Refs. 9, 10) for no clearly understood reasons. Assuming sufficient altitude is available, flight tests show that recovery from the VRS is usually attained quickly by the application of cyclic control inputs to increase the in-plane component of velocity at the rotor, thus sweeping the recirculating wake away from the rotor disk.

Several researchers have studied the VRS using rotors under more controlled laboratory conditions (Refs. 1, 7, 11–15). The work of Drees & Hendal (Ref. 1) contains the most comprehensive flow visualization of the VRS to date. Washizu et al. (Ref. 12) have made extensive quantitative measurements of rotor performance (thrust and power) when operating in the VRS. Their data includes measurements under VRS conditions with the rotor in inclined descending flight. Yaggy & Mort (Ref. 13) have shown that the unsteady airloads produced in the VRS depend on rotor disk loading, confirming the nonlinearity of the aerodynamic behaviour of the rotor in the VRS. Recently, Betzina (Ref. 7) has conducted experiments in descending flight conditions with a relatively highly loaded rotor representative of that used on a tiltrotor.

Various inconsistencies between these experimental studies suggest that a deeper look into the physics of the VRS is required. The relatively sparse experimental work on the VRS has thus far been paralleled by limited modelling efforts, in the first instance by using forms of momentum theory or semi-empirical extensions thereof (Refs. 3, 4, 16–18). A limitation with the momentum theory is that it cannot strictly be applied in the VRS because of the ambiguity in defining a control volume over which to apply the governing equations (Ref. 19). Also, it does not provide any indication of the effects of rotor geometric parameters (number of blades, rotor solidity, blade planform or blade twist etc.) or rotor configuration (conventional, side-by-side, tandem, overlapping etc.) on the physics of the VRS. This is a significant deficiency that must be treated by more advanced mathematical models. Nevertheless, despite its fundamental limitations, experience has shown that momentum theory (with empirical guidance) can provide a good level of engineering capability in establishing the bounds of the likely VRS envelope for single rotors (Ref. 3).

It has been suggested (Refs. 5, 6) that the physics behind the onset of the VRS is related to the susceptibility of the rotor wake vortices to Kelvin wave-type instability. The growth of Kelvin waves to appreciable amplitudes may be the precursor to the nonlinear growth mechanism that eventually leads to rotor wake breakdown in the VRS. The problem of wake stability has been examined under various operating conditions using a linearized, eigenvalue analysis of the rate of growth of perturbations to the vortical structure of the rotor wake (Ref. 5). The stability analysis suggests that the helicopter rotor wake is inherently unstable in most flight regimes, including in hover, and shows that increasing the rate of descent makes the wake more prone to instability. Interestingly, blade twist adversely affects the stability of the wake through its effect on the induced velocity distribution near the rotor.

The results described in the following sections confirm that the location of the boundary of the VRS depends on a tradeoff between various wake parameters that are influenced by the geometry of the rotor blades. In addition, the level of the fluctuations of operating parameters, such as thrust and torque, experienced by the rotor within the VRS appears to be sensitive to the level of twist used on the rotor blades. Blade twist has two effects. Firstly, the overall distribution of induced velocity at the rotor is sensitive to blade twist. Secondly, blade twist affects the local sectional lift coefficients on the rotor. For high blade twist, the local lift coefficients may become large enough for the inboard sections of the rotor to stall. The effects of flow separation may be significant even at low thrust coefficients, but at high thrust coefficients where the rotor may be stalled over a more appreciable fraction of its area, rotors with and without significant blade twist show marked differences in their behaviour under VRS conditions.

Numerical Methodology

Engineering Model

Newman et al. (Ref. 3) have developed an engineering model for predicting the location of the VRS boundary for a single-rotor helicopter. The model relies on the observation, mentioned earlier, that all helicopter wakes are inherently unstable and thus that disturbances in the vortex structure laid down by the rotor blades will grow as the wake is convected downstream of the rotor. The engineering model is based on a heuristic explanation for the onset of VRS conditions in terms of the rate of growth of these disturbances relative to the rate at which the growing disturbances are convected downstream of the rotor. The rate of growth of the disturbances is proportional to the strength of the wake vorticity, and hence to the rotor thrust. The rate of convection of the disturbances downstream into the rotor wake is governed by the induced velocity as well as the forward speed and descent rate of the rotor.

For most combinations of descent rate and forward speed, disturbances to the rotor wake generally grow to appreciable magnitudes far enough downstream from the rotor for them to have negligible effect on blade airloads and rotor response. On the other hand, if the rate of convection in the wake is small enough so that disturbances grow to appreciable magnitudes close to the rotor, then the unsteadiness associated with these wake structures will have a more appreciable effect. The situation is exacerbated by the coupling between the production of perturba-

tions in the wake structure and any unsteadiness induced in the blade airloads by interactions with the wake. In fact, it is likely that this feedback is at the heart of the nonlinear growth mechanism that leads to the eventual breakdown of the wake in the VRS. The engineering model visualizes the rotor as entering the VRS under certain combinations of forward speed and descent rate as the rotor is engulfed within the physical products of the wake instability. Independent calculations using CFD-based (Ref. 3) and free-vortex wake (Refs. 5, 6) approaches to modelling the unsteady aerodynamics of the rotor wake clearly support this hypothesized mechanism for the onset of the VRS.

Mathematically, the engineering model relies on conventional actuator disk theory to define a critical rate of transport $\overline{\mu}_W$ of the products of the wake instability into the wake downstream of the rotor. At this critical rate of transport, the rotor wake breaks down yielding the VRS. Expressing this critical rate in terms of the free-stream velocity components $\overline{\mu}_x$ and $\overline{\mu}_z$ and the mean induced velocity $\overline{\lambda}_i$ at the rotor disk gives

$$\overline{\mu}_W^2 = (k\overline{\mu}_x)^2 + (\overline{\mu}_z + \overline{\lambda}_i)^2 \tag{1}$$

where the overbars indicate that the various velocity components have been scaled by the hover induced velocity, λ_h. Using this scaling, pairs $(\overline{\mu}_x, \overline{\mu}_z)$ satisfying this relationship define a boundary for the onset of the VRS that is universal, in the sense that it applies to isolated rotors operating over a wide range of thrust coefficients.

This simple model gives reasonably good general agreement with previously published experimental studies of the VRS boundary, as shown in Ref. 3. One of its most important predictions is that rotors with higher disk loadings should become susceptible to the VRS at higher forward speeds, and over a broader range of descent rates, compared to rotors with low disk loading. An empirical value of 0.65 for the parameter k can be supported analytically by considering the relative effectiveness of the in-plane and out-of-plane velocity components at the rotor disk in transporting the vortical products of the wake instability away from the rotor (Ref. 4). On the other hand, the value of $\overline{\mu}_W$ can, at present, be determined only by comparison with experimental data, or from the predictions of numerical methods that track the wake vorticity in a fully time-accurate manner.

As to be expected from a model that has its foundations in the classical momentum theory for rotors, the principal limitation of this model is that it cannot predict the effects of changes in the details of the rotor design, such as the level of blade twist, taper, or changes in aerofoil properties along the length of the blades. The new results shown in the present paper suggest that this momentum-based theory could (and should) be extended with guidance from more advanced numerical models to enable routine engineering predictions of the factors that influence the onset of the VRS.

Wake Stability Theory

A full understanding of the flow conditions that cause the wake of the rotor to collapse into the disordered, recirculating flow that is characteristic of the VRS is key to understanding the onset of the phenomenon. Insight into the mechanism of collapse, and into the effect of details of the rotor design, can be obtained from a linear analysis of the rate of growth of perturbations applied to a range of equilibrium wake structures.

It is a fundamental property of incompressible, irrotational fluids that any embedded vorticity will be freely convected by the surrounding fluid. The motion of any wake element is then governed by the simple advection equation

$$\frac{d\mathbf{r}}{dt} = \mathbf{V}(\mathbf{r}), \quad \mathbf{r}(0) = \mathbf{r}_0 \tag{2}$$

where $\mathbf{r}$ is the position of a point on the vortex wake, $\mathbf{r}_0$ is the initial position of the point, and $\mathbf{V}(\mathbf{r})$ is the local fluid velocity.

Eigenvalue analysis of the stability of the wake begins by obtaining a basic equilibrium solution for the rotor wake geometry, for instance by solving Eq. 2 using a free-vortex method (Refs. 5, 20, 21). The equilibrium solution is then perturbed by a small quantity $\delta\mathbf{r}$. The evolution equation for the perturbed wake geometry $\mathbf{r} + \delta\mathbf{r}$ is then

$$\frac{d(\mathbf{r} + \delta\mathbf{r})}{dt} = \mathbf{V}(\mathbf{r} + \delta\mathbf{r}) \tag{3}$$

If the equilibrium equation (Eq. 2) is subtracted from Eq. 3 and the higher-order terms in $\delta\mathbf{r}$ are neglected, the linearized evolution equation

$$\frac{d(\delta\mathbf{r})}{dt} = \delta\mathbf{V}(\delta\mathbf{r}) \tag{4}$$

for the wake perturbation $\delta\mathbf{r}$ is obtained.

Any arbitrary small perturbation to the wake can be represented as a series of normal modes. In cylindrical coordinates, the perturbation modes have the form

$$\{\delta\mathbf{r}\} = \left\{ \begin{array}{c} \delta r_0 \\ \delta\theta_0 \\ \delta z_0 \end{array} \right\} e^{\alpha t + i\omega\zeta} \tag{5}$$

where α is the growth rate and ω is the wave number of the mode; that is, the perturbation wave has ω cycles for each rotor revolution. Equation 4 can then be solved for each perturbation mode at any given point on the wake, say P. After some manipulation, the solution can be reduced to the standard eigenvalue form

$$\alpha_P \{\delta\mathbf{r}\}_P - [M]_P \{\delta\mathbf{r}\}_P = 0 \tag{6}$$

The eigenvalues α_P give the growth rate of the perturbation mode $\{\delta\mathbf{r}\}_P$ at point P. A positive eigenvalue corresponds to an unstable mode.

It has been shown using this approach (Ref. 5) that the stability of the rotor wake depends on both the rotor geometric configuration (i.e., number of blades, blade twist, number and placement of rotors, etc.) as well as the operating state of the rotor (i.e., thrust and rate of descent). While

a linearized stability analysis allows rigorous examination of the factors that determine the *onset* of wake instability, like the engineering model described earlier, it cannot provide a means of predicting what happens *after* the wake has become unstable. The non-linear evolution of the unstable wake must be tracked using numerical methods that model the dynamics of the wake vorticity in a fully time-accurate manner. Later in this paper, results from two such approaches, namely the Vorticity Transport Model (VTM) and the Free Vortex Model (FVM), are presented.

Vorticity Transport Model (VTM)

The most fundamental representation of the wake of the rotor is as a time-dependent vorticity distribution in the region of space surrounding the rotor. If $\mathbf{V}$ is the flow velocity, then the associated vorticity distribution $\omega = \nabla \times \mathbf{V}$ evolves according to the unsteady vorticity transport equation

$$\frac{\partial}{\partial t}\omega + \mathbf{V}\cdot\nabla\omega - \omega\cdot\nabla\mathbf{V} = \mathbf{S} \tag{7}$$

This equation can be derived from the Navier-Stokes equations under the assumptions of incompressibility and in the limit of vanishing viscosity (Ref. 23), and shows the rotor wake to arise as a vorticity source $\mathbf{S}$ associated with the generation of aerodynamic loads on the rotor blades. The differential form

$$\nabla^2\mathbf{V} = -\nabla\times\omega \tag{8}$$

of the Biot-Savart relationship relates the velocity at any point near the rotor to the vorticity distribution in the flow, and hence allows the geometry and strength of the rotor wake to feed back into the aerodynamic loading and blade response.

The Vorticity Transport Model (VTM) developed by Brown (Ref. 23) employs a direct computational solution of Eq. 7 to calculate the evolution of the wake of the helicopter. The model is capable of representing blade-wake interactions, as well as the wake-wake interactions that lead to the growth, coalescence and rupture of vortical structures in the rotor wake, and thus embodies a high level of physical realism. The VTM is coupled into the blade dynamic simulation of the rotor by using the loads generated by the rotor aerodynamic model to construct $\mathbf{S}$ in terms of both the shed and trailed vorticity from the blades.

After casting the equations on a structured Eulerian computational grid surrounding the rotor, Eq. 8 is solved by cyclic reduction (Ref. 24), while Eq. 7 is marched through time using Toro's Weighted Average Flux algorithm (Ref. 25). Most CFD-type approaches currently in use suffer excessively from numerical dissipation of vortical structures in the rotor wake. This renders them effectively useless for VRS calculations where the recirculating nature of the flow causes vortical structures to persist near the rotor for very long times. The advantage of using the Weighted Average Flux algorithm to calculate the evolution of Eq. 7 is that very tight control can be maintained over the rate of dissipation of vorticity in the wake, and so vortical structures retain their strength and geometry even though their interactions with the rotor may continue over many rotor revolutions.

Although the VTM provides a very complete model for the evolution of the structure of the rotor wake under VRS conditions, it is computationally expensive for routine parametric studies of the detailed effects of blade design on the behaviour of the rotor in the VRS. For these purposes, computational methods that trade some resolution of the detail of the rotor wake against improved computational efficiency must be used. One successful such method is the Free-Vortex Model (FVM).

Free-Vortex Model (FVM)

The FVM uses a Lagrangian description of the flow. Discrete line vortices are used to represent the structure of the rotor wake, and, as described previously, the motion of markers attached to these lines is described by Eq. 2. In a typical application of the FVM, markers are placed at equal intervals of time along vortex filaments trailed from the rotor blades, and are linked together using a piecewise-linear reconstruction. In a blade fixed coordinate system, Eq. 2 becomes the partial differential equation

$$\frac{\partial\mathbf{r}}{\partial\psi} + \frac{\partial\mathbf{r}}{\partial\zeta} = \frac{\mathbf{V}(\mathbf{r})}{\Omega} \tag{9}$$

where ψ is the azimuthal location of the blade, and ζ is the age of the vortex marker relative to the blade azimuth when it originated. The left-hand side of Eq. 9 is an advection equation with a temporal direction ψ and a spatial direction ζ. The numerical solution of Eq. 9 proceeds by time-marching after the partial derivatives have been approximated using finite differences. Because most standard numerical integration schemes exhibit some type of non-physical instability if used to advance Eq. 9, special integration schemes must be developed to preserve both the temporal accuracy and the stability of the method (Ref. 26). The present approach uses Bhagwat & Leishman's PC2B scheme, which has a five-point central difference approximation to the spatial (ζ) derivatives, and a three-point second-order backward difference approximation to the temporal (ψ) derivatives. The PC2B scheme is specially designed to introduce truncation terms that are dissipative, so balancing and stabilizing the governing equations for the wake while retaining its overall second order accuracy. The velocity field $\mathbf{V}$ is evaluated by applying the Biot-Savart law to all the vorticity being shed and trailed from the blades, and for straight-line segmentation this approach is spatially second-order accurate (Ref. 27).

Interpretation of Calculations

Before proceeding to the results of calculations of the VRS performed using the numerical models just described, some remarks on the limitations of their interpretation are in order. The computational models attempt to provide time-accurate descriptions of a highly-unstable, nonlinear, time-dependent flow that, especially under incipient VRS conditions, takes significant time to develop fully. It is

inevitable under these circumstances that divergences in detail will emerge relatively rapidly in the predictions of computational models as a result of even very small differences in their construction, let alone as a result of the large differences in the approaches taken by the VTM and the FVM.

In particular, small changes in modelling assumptions or initial conditions may result in significantly different instantaneous patterns of flow development, such as revealed in the snapshots of the wake structure presented in the next section, and thus in the detailed time-histories of the loads experienced by the rotors. Overly direct comparison of the predictions of the VTM and the FVM on the basis of a limited number of data points is extremely risky, and, for this reason, the analysis of the results presented in the following sections focuses on exposing the *global* (and, hence, hopefully, model-independent) characteristics of the VRS that are predicted by both computational models.

Finally, because of the computational demands of time-accurate calculations, the results presented in this article are based on accelerated flight conditions in an effort to cover a broad range of flight conditions in a single calculation. As will be discussed more fully later in this paper, it is possible that, under these circumstances, effects induced by the flight path of the rotor and the time delays in the development of the wake could introduce significant variations in the rotor and wake behaviour from those observed under quasi-steady flight conditions.

Results & Discussion

Linearized Wake Stability Analysis

Insight into the susceptibility of the wake to instability, and hence to the factors influencing the onset of the VRS, can be obtained from a linear analysis of the rate of growth of perturbations to the wake, as outlined earlier. Figure 2 shows results for a four-bladed rotor operating at constant thrust in axial flight over a range of climb or descent speeds. The equilibrium wake structures, on which the results of this section are based, were obtained using the FVM. In particular, the equilibrium structure of the wake was approximated by the converged geometry of the trajectories of the blade-tip vortices alone. In each case, the blade loading was kept constant at $C_T/\sigma = 0.075$ to yield results for wakes with nominally the same tip vortex strengths. The results suggest the rotor wake to be inherently unstable in all cases. The fastest-growing perturbations to the wake structure are associated with disturbances with wave numbers equal to half-integer multiples of the number of blades.

Figure 2 shows the expected decrease in wake stability that results from the reduction in the helicoidal spacing between the vortex filaments in the rotor wake as the descent rate of the rotor is increased. Notice too that the descending rotor exhibits a substantial increase in the growth rate of disturbances with higher wave numbers when compared to the same rotor in hover. This implies an increased susceptibility to wake instability triggered by small-scale disturbances in the flow, and suggests that the onset of the VRS may be triggered by BVI at the rotor or by atmospheric turbulence rather than by larger-scale disturbances in the surrounding flow. This fact may prove to be an important impediment to the achievement of converged and reliable numerical predictions for the onset of the VRS.

An important factor affecting wake stability is the distribution of thrust along the length of the rotor blades. This is governed primarily by blade twist, and, to a lesser extent, by blade planform. The thrust distribution affects the induced velocity at the blades and the distribution of the induced velocity in the far wake. The axial settling rate of the tip vortices in the far wake (which is essentially the wake helicoidal spacing for a fixed number of blades) increases with the square-root of rotor thrust, but is also affected by the rotor thrust distribution along the rotor blades. This is because increasing (nose-down) blade twist progressively off-loads the tip region, reducing the induced velocity there and decreasing the velocity at which the wake vorticity is convected away from the rotor. It is also known that the effect of blade twist on the axial settling rate becomes more significant for rotors that operate at high disk loadings.

The general effect of blade twist on the stability of the wake is shown in Fig. 3. Results are given for four-bladed

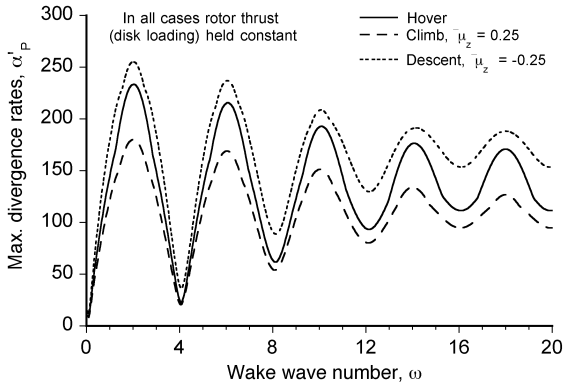

Figure 2: *Effect of climb or descent velocity on the maximum non-dimensional wake perturbation growth rates for a 4-bladed rotor.*

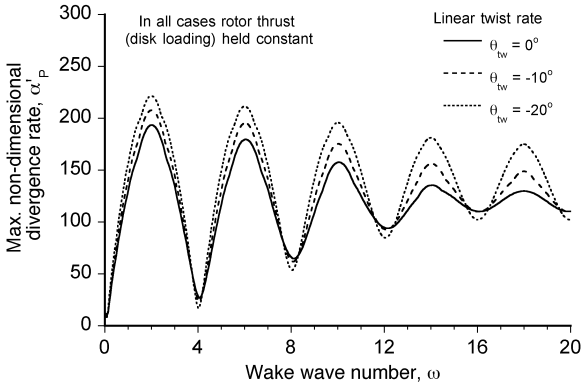

Figure 3: *Maximum non-dimensional wake perturbation growth rates for a 4-bladed rotor operating at constant thrust but with different linear blade twist rates.*

rotors operating at the same disk loading but having various linear blade twist rates. The divergence rates are normalised by the tip vortex strengths in order to emphasise the geometric effects of twist rate. When compared on this basis, rotors with high nose-down blade twist are found to be more prone to wake instability compared to rotors with low blade twist. In fact, as twist increases, the tip vortex strength reduces slightly, reducing the tendency for the wake of the twisted blade to instability, but rotor blades of unconventionally high twist emerge from the analysis with a noticeable tendency toward early wake breakdown when compared with more conventionally twisted rotor blades. Results obtained using the time-accurate numerical methods described earlier will now be presented to explore these ideas further.

Rotor Thrust and Torque Response

The thrust and torque generated by a three-bladed rotor in trimmed descent along a flight path passing through the VRS have been calculated using both the VTM and the FVM. The selection of flight cases presented in this section acknowledges the fact that pilots encounter the VRS more commonly when the helicopter is descending with a component of forward velocity.

Results, plotted against the descent velocity of the rotor (scaled by the hover induced velocity given by momentum theory), are shown in Fig. 4. Two cases are shown: in the first case, the blades have a linear twist of 8° to be representative of historical helicopter design practice, while in the second case the blades have a much higher twist of 35°. In both cases, the rotor was maintained on a 65° glideslope and given a vertical acceleration $d\overline{\mu}_z/dt = -0.03$ per rotor revolution. The consequences of adopting an accelerated flight path through the VRS, albeit even at a very low rate, will be discussed later in this paper. In both cases the collective and cyclic pitch settings on the rotor were continually adjusted to maintain a nominally constant thrust coefficient of 0.00362 and approximately zero cyclic flapping with respect to the rotor shaft.

For the rotor with moderately twisted blades, the VTM predicts a regime of moderate thrust fluctuations at very low descent rates to precede a sudden increase in intensity at a descent rate $\overline{\mu}_z \approx 0.5$. Similar calculations show the thrust generated by the rotor with highly twisted blades to be quiescent until a moderate descent rate is attained. In contrast, the FVM predicts the thrust generated by the rotor with moderately twisted blades to be quiescent until moderate descent rates are attained, while similar calculations for the rotor with highly twisted blades predict intense thrust fluctuations to begin almost as soon as the rotor begins to descend. The maximum amplitude of the thrust fluctuations predicted by the VTM is about 15% of the mean thrust of the rotor, and the signal consists of a strong vibratory component (at greater than 1/rev) superimposed on an erratic thrust variation at frequencies low enough to affect the flight dynamics of the rotorcraft. For the rotor with highly twisted blades, the FVM predicts thrust fluctuations with similar amplitude to those predicted by the

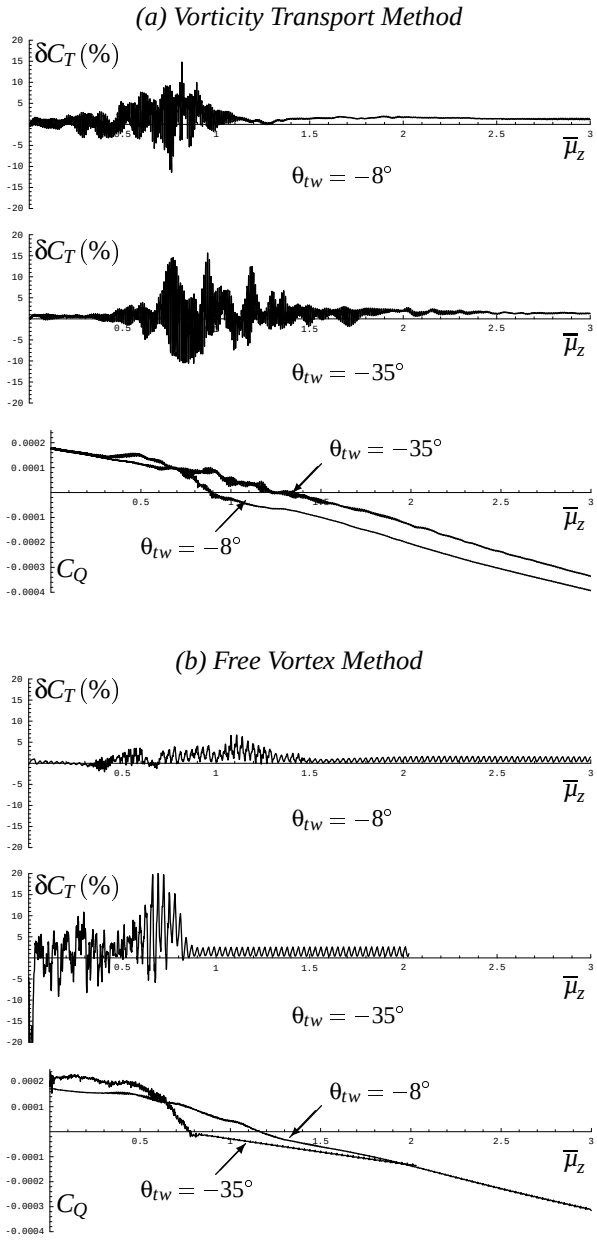

Figure 4: *Predicted thrust perturbations and torque coefficients for an isolated rotor,* $C_T = 0.0036$*, on an accelerated* 65° *glideslope passing through the VRS.*

VTM, but fluctuations with significantly lower amplitude are predicted for the rotor with moderately twisted blades. Notice also that the two numerical methods predict significantly different ranges of descent rate over which the thrust fluctuations persist, once established, for the two rotors with different twist rates.

If the onset of the thrust fluctuations experienced by the rotors is interpreted in an overly simplistic way to indicate directly the onset of VRS conditions, then the results presented here appear to contradict each other, and, indeed, to contradict the predictions of the linear stability analysis of the rotor wake presented earlier. It can be argued though that the content of the thrust signal at frequencies higher than 1/rev is not an essential component of the VRS. It is common piloting knowledge that a high vibrational com-

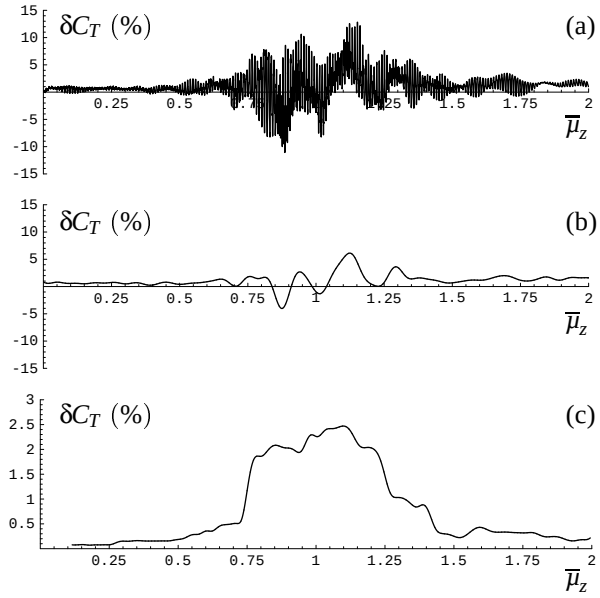

Figure 5: *Thrust perturbations for an isolated rotor, nominal* $C_T = 0.0036$, $\theta_{tw} = -35°$, *predicted by the VTM along an accelerated* 70° *glideslope passing through the VRS. (a) Thrust perturbation (%), (b) Filtered thrust, and (c) Standard deviation of thrust.*

ponent to the thrust response of the rotor may be encountered under a wide range of descent conditions that are not usually considered to be within the VRS. These thrust fluctuations usually result from localized BVI events as the rotor wake is forced up against (or even through) the rotor disk. This can occur without the wake necessarily being subject to incipient VRS. On the other hand, the presence of low-frequency variability in the thrust generated by the rotor should be a much more reliable indicator of the onset of the VRS since this is most likely associated with the erratic motions of the collapsed rotor flowfield.

Figure 5 shows the thrust response of the rotor after filtering to remove all frequency components at greater than 1/rev. This figure exposes the low-frequency variability of the rotor thrust response that is found over the relatively narrow band of descent rates usually associated with the VRS. Some illumination on the character of the nonlinear growth mechanism implicated in the breakdown of the rotor wake in the VRS can also be gleaned from the thrust data presented here. Weak nonlinearity in conjunction with the postulated initiation mechanism in terms of the growth of linearly unstable perturbations to the wake structure would manifest in a plot of thrust coefficient versus descent rate as a gradual onset of VRS-like conditions as the vortical structures produced by the onset of wake instability gradually reached the rotor. This situation would imply that the location of the VRS onset boundary could be defined in an essentially arbitrary manner, for instance simply by selecting an appropriate threshold value for perturbations to the thrust coefficient. In Fig. 5(c) the standard deviation from the mean of the filtered thrust signal, sampled on a moving time-window two rotor revolutions wide, is plotted against the rotor descent rate. The sharp-edged plateau-like appearance of the thrust response processed in this way is significant, and supports the idea that the onset of VRS is not gradual, but is associated with a catastrophic, or at least a very sudden, loss of stability in the rotor wake. Previous numerical simulations have shown (Refs. 3, 5, 6) that the onset of VRS in axial flight is associated with a highly nonlinear axial symmetry-breaking transition in the wake, but in the inclined descent case presented here, the situation must necessarily be more complex.

Figure 6 shows a re-analysis of the thrust variations predicted by the VTM and the FVM using the windowed standard deviation of the thrust signal to determine the onset of the VRS. Note that the data has been scaled to account for the difference in the amplitude of the thrust variations predicted by the two methods. This scaling has no effect on the outcome of the analysis if the onset of the VRS is identified simply by the descent rate at which a sharp rise in the amplitude of the standard deviation of the thrust signal is observed. Using this measure, the agreement between the descent rates predicted by the VTM and the FVM for the onset of the VRS is striking, particularly in the calculations for the rotor with moderate twist. The calculations for the rotor with high twist, on the other hand, show just how complicated the rotor's behaviour in descending flight can be. Comparison with the predictions of the VTM shows that the second peak in the FVM-generated signal (i.e. the peak at higher descent rate) is most likely the one to be correctly associated with the VRS. The earlier peak in the signal could quite conceivably be a feature of very strong BVI on the rotor as descent is initiated.

It remains to explain the discrepancies in the predicted duration, once established, of VRS conditions on the rotor as the descent rate is increased. Valuable insight into the differences in rotor behaviour predicted by the two models, and also into the effects of blade twist on the behaviour of the rotor in the VRS, can be obtained by correlation of the observed thrust response with the behaviour of the flow in the wake of the rotor. Figure 7 shows representative contour plots of the vorticity magnitude predicted by the VTM for the 65° descent case described above. The flow in a longitudinal plane passing through the rotor shaft is shown. These plots represent a snapshot of the wake struc-

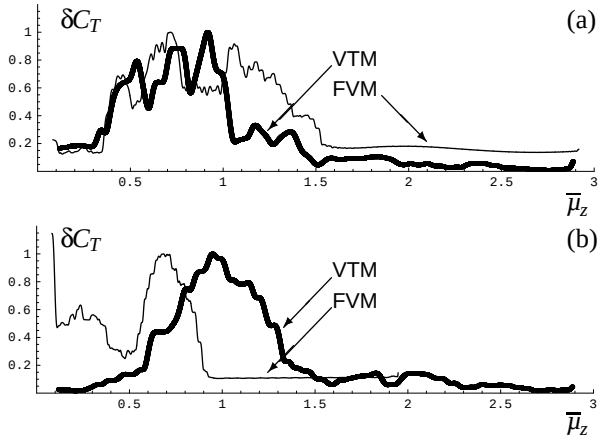

Figure 6: *Standard deviation of the thrust perturbations for an isolated rotor, nominal* $C_T = 0.0036$, *along an accelerated* 65° *glideslope passing through the VRS. (a)* $\theta_{tw} = -8°$, *(b)* $\theta_{tw} = -35°$

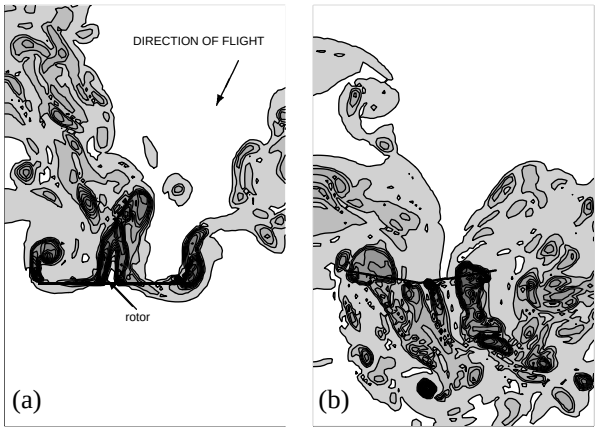

Figure 7: *Vorticity distributions in a longitudinal plane surrounding the rotor as predicted by the VTM in descending flight when* $\overline{\mu}_z = -0.8$ *and* $C_T = 0.00362$*: (a)* $\theta_{tw} = -8°$*, (b)* $\theta_{tw} = -35°$.

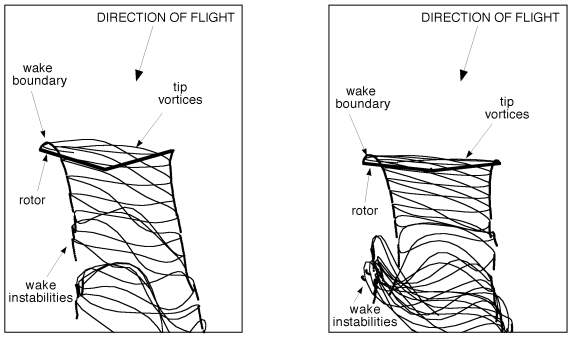

Figure 8: *Side view of wake geometry and intersections of vortex filaments in a longitudinal plane (wake boundary) as predicted by the FVM in descending flight when* $\overline{\mu}_z = -0.8$ *and* $C_T = 0.00362$*: (a)* $\theta_{tw} = -8°$*, (b)* $\theta_{tw} = -35°$.

ture with the rotor deeply in the VRS, at a descent rate $\overline{\mu}_z = -0.8$. Figure 8 shows the corresponding wake structures generated by the FVM and locates the positions of the wake filaments as they intersect the same longitudinal plane (indicated in Figure 8 as the 'wake boundary').

While the VTM and the FVM predict very clear differences in the structure of the wake under VRS conditions, it is apparent in all cases that the methods do predict the accumulation of vorticity near the plane of the rotor that has been shown (see Fig. 1) to be a characteristic feature of the wake's geometry in the VRS. Also apparent in the calculations is the strong recirculation of ambient vorticity through the rotor disk. The results from the VTM suggest that, for the particular flight trajectory represented here, some of this vorticity originates from earlier passage of the rotor through its own wake.

Some of the differences in the predictions made by the VTM and the FVM can be attributed to the different levels of fidelity inherent in the two models. In the case of the VTM, the vorticity in the wake originates from the shed and trailed vorticity generated along the entire length of each of the rotor blades. The FVM tracks only the vorticity trailed from the blade tips. It is apparent from Fig. 7 that significant vorticity is generated by the blade root and hub region; this feature of the flow is simply not captured by the FVM. It is known that the geometry of the wake observed at any particular instant while in the VRS is extremely sensitive to the detailed history of its prior evolution (an issue to be discussed more fully later in this paper). It is plausible that the dynamics of the wake vorticity originating from the portions of the blade inboard of the tip could thus have a very strong effect on the evolution of the wake leading up to and through the VRS.

Further evidence of the importance of the vorticity originating from the inboard sections of the rotor blades in governing the behaviour of the rotor in the VRS is provided by the absence of a consistent dependence on twist rate in the plots of torque coefficient against descent rate shown in Fig. 4. It is known that the location and relative size of the regions on the rotor in which power is either consumed or absorbed is very strongly governed by blade twist, but also by the details of the inflow distribution over the rotor disk. The inflow distribution is, of course, strongly governed by the distribution of vorticity in the near wake. Noteworthy in this figure is the dependence of the rate of descent that the rotor would adopt in autorotation (with $C_Q \approx 0$) on the twist of the rotor blades. Note too the sudden decrease in the slope of the variation of torque coefficient with descent rate which is predicted by the FVM to occur, for the rotor with highly twisted blades, at a descent rate slightly greater than that adopted by the rotor in autorotation. This indicates the onset of rotor stall – a subject that is discussed more fully in a later section of this paper.

The most interesting feature, though, of the comparison between the wake structures generated by the two numerical models is that both the VTM and the FVM predict the wake structure generated by the rotor with highly twisted blades to be significantly different to that generated by the rotor with moderately twisted blades, even when examined under exactly the same flight conditions. Clearly, the details of the loading distribution along the rotor blades, and the associated distribution of vorticity that is created in the rotor wake, must play a strong role in governing the precise dynamics of the rotor wake, and hence the unstable growth of disturbances in the rotor wake and its eventual breakdown into the VRS. The loading distribution on the blades is, of course, strongly governed by their twist.

Vortex Ring Envelope

The time-accurate VTM or FVM models can be used to map out the regions of the flight envelope where the rotor might be prone to entering the VRS. Knowledge of the location of the onset boundary of the VRS can be important for several operational reasons, including the fact that at low airspeeds it may be necessary for the rotorcraft to pass through the VRS, albeit briefly, to enter into equilibrium autorotational flight. The onset boundary of the VRS can be identified, for example, by sequentially mapping out combinations of rotor operating conditions such as flight path angle, descent velocity or forward speed where the rotor experiences high fluctuations in thrust, shaft torque or

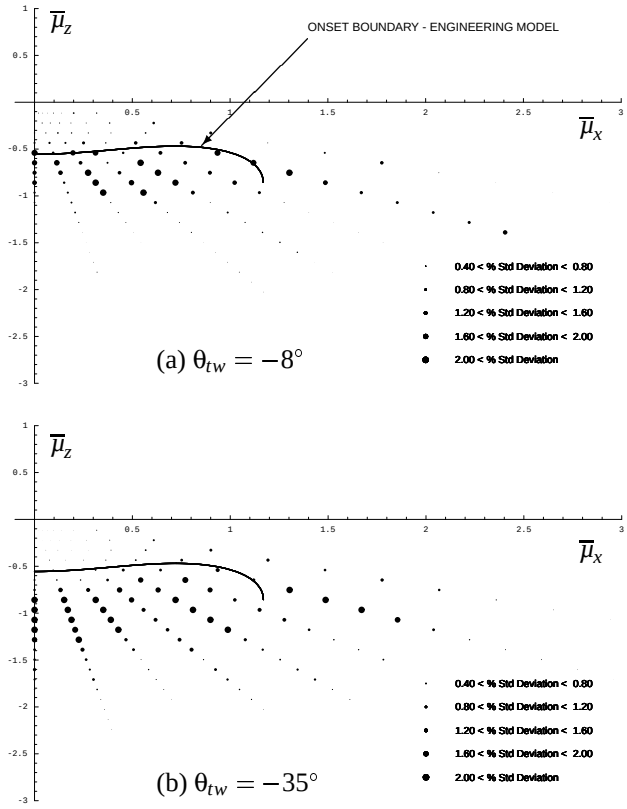

Figure 9: *Vortex ring onset for an isolated rotor as predicted by the VTM: (a)* $\theta_{tw} = -8°$*, (b)* $\theta_{tw} = -35°$.

blade flapping. This strategy is typically adopted in wind tunnel experiments or flight test. However, in flight tests there may be considerable uncertainties in this process, including those induced by piloting difficulties in maintaining equilibrium flight at or near to the VRS, the possible existence of non-unique operating states, and also a dependence (as will be discussed later) on the manner in which the VRS flight condition is approached.

In Fig. 9, the windowed standard deviation of the filtered thrust response of the rotor is used as an indicator of the onset of the VRS. In the figure, the standard deviation of the thrust signal predicted by the VTM is plotted for a range of descent angles between 0° and 90° with the rotor operating at a nominal thrust coefficient of 0.00362. The largest circles denote flight states within the VRS as indicated by the windowed standard deviation of the rotor thrust response exceeding a threshold of 2% of the nominal operating thrust coefficient of the rotor. Differences in the shape, extent and positioning of the VRS on the diagram of descent rate versus forward speed are apparent for the two rotors with differing blade twist. While the VTM predicts the onset of the VRS to occur at slightly higher rates of descent for the the rotor with the more highly twisted blades, it is significant to note, in the context of the linear stability analysis of the rotor wake, that the rotor with highly twisted blades is susceptible to the VRS over a much larger range of conditions than the rotor with moderately twisted blades.

The onset boundary of the VRS predicted by the simple engineering model (when the VRS is approached by increasing the descent rate of the rotor) is shown in Fig. 9 by plotting the low–$\overline{\mu}_z$ branch of solutions to Eq. 1. The value $\overline{\mu}_W = 0.76$ used to generate this boundary was previously established (Ref. 3) by comparison with published experimental data, principally for rotors with low to moderate blade twist. Not unsurprisingly, the numerical data for the onset of VRS for the rotor with moderately-twisted blades agrees well with the results of the engineering model. When the presence of VRS effects is judged by the same measure for the rotor with highly-twisted blades, however, somewhat different results are produced, with a general widening of the envelope where VRS might be expected to occur. This effect cannot be incorporated into the engineering model by a simple change in parameters that remains consistent with the physical basis of the model. Yet, the results presented here suggest that an extension of the model, using both the VTM and the FVM for guidance in its construction, should be well capable of taking the effects of blade twist into account.

To meet this goal, two points are important to bear in mind. The first is that the engineering model is based on classical momentum theory, and so requires a well-defined stream tube to exist in the wake of the rotor. For this reason the model is strictly invalid within the VRS, and so cannot yield insight into the eventual cessation of VRS effects as the descent rate of the rotor is further increased. The second important point is that, because the numerical data used to construct the diagrams is obtained under accelerated flight conditions, the numerically-reconstructed onset boundary for the VRS represented here is an approximation to the boundary that would be obtained under more generally-applicable conditions of constant descent rate. It was shown in previous numerical simulations (Ref. 3) that accelerated flight conditions (admittedly at very much higher rates than used in the present calculations) could suppress the onset of VRS to the extent that, at very high accelerations, the rotor could be forced through a sequence of transient states so quickly that no vortex ring state could be discerned from the thrust response of the rotor. Further, the imposition of certain accelerated manoeuvres, such as sharp pull-ups, have been shown (Ref. 6) to cause the rotor to encounter the symptoms of VRS at combinations of descent rate and airspeed where the VRS would not normally be expected.

Indeed, a complication in fully understanding the highly nonlinear flow physics of the VRS, and in predicting the VRS flight boundaries, is that the onset of the VRS appears to be flight path dependent. In other words, the flow conditions and transient airloads produced on the rotor in the VRS depend on the both the initial rotor operating conditions and on the manner in which the VRS is approached. Furthermore, subsequently reversing the combination of airspeed and rate of descent back to the initial flight condition may not yield the same time-history of the airloads – there is a hysteresis effect. The situation is illustrated in Fig. 10. As an example, increasing the rate of descent at a constant airspeed (as along path AC in Fig. 10) may not give the same wake dynamics and rotor airloads when point C is finally reached as if the same flight condition

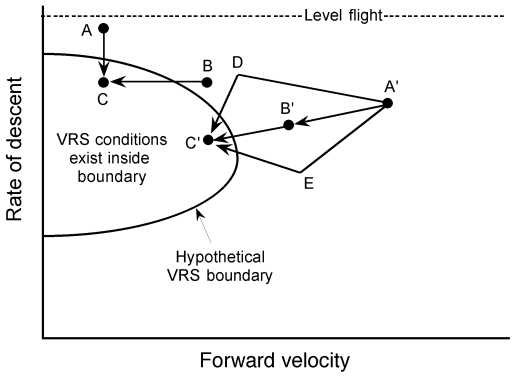

Figure 10: *Dependence on flight path may determine the final aerodynamic operating conditions of the rotor when operating near VRS.*

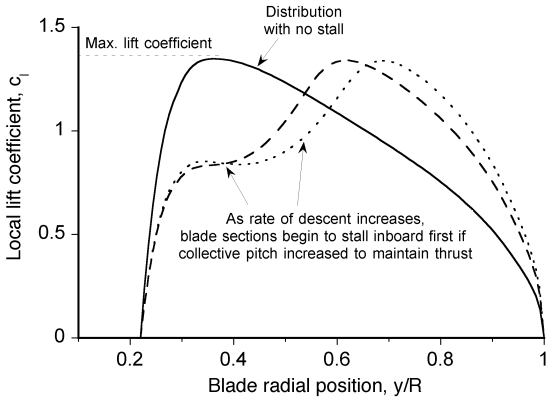

Figure 11: *Representative spanwise distributions of local lift coefficients for a rotor in an incipient VRS condition showing evidence of stall inboard on the blades.*

is approached by changing the airspeed at a constant rate of descent (as along path BC in Fig. 10). This type of behaviour is seen in the flight test data of Scheiman (Ref. 8), and has been noted by Varnes et al. (Ref. 2) but without explanation. With minimal extrapolation, the observed dependence of the rotor behaviour, at any particular instant, on the flight states it has experienced in its past could explain why it is possible, as postulated earlier, for the rotor to reach more than one final (but nominally equilibrium) flow state at any particular combination of descent rate and forward speed.

In many cases, however, the behaviour of the rotor (for instance at point C) may evolve towards essentially a single state, independently of the initial condition of the rotor, if the flight conditions are maintained for a sufficiently long time after reaching the final operating point. Yet, because of the inherently long time lags associated with adjustments within the rotor flow field, the final state of the rotor may take many rotor revolutions to develop. This is usually not the case for flight conditions sufficiently far away from the VRS boundary, for instance when the path A'B' shown in Fig. 10 is followed. In this case, the final flow conditions at point B' would be expected to be essentially independent of the path taken to reach it. However, different flow conditions may be expected when following paths A'C', A'DC' or A'EC'. From a computational perspective, these effects may manifest themselves as a strong dependence of the details of the predicted rotor loads and wake geometry on the fidelity of the computational model, as postulated earlier in this paper. While a fuller discussion of these effects is outside the scope of the present article, it is important to appreciate that, issues of model fidelity notwithstanding, the sensitivity of the rotor behaviour to initial conditions, and the presence of aerodynamic effects which are dependent on the path, rate, and acceleration of the rotor, complicate significantly the complete understanding and prediction of rotor behaviour in the VRS. These issues must carry over to any attempts to determine VRS boundaries from wind tunnel measurements, and especially from flight tests.

Role of Blade Stall in VRS

Earlier it was shown that, under incipient VRS conditions and within the VRS itself, the rotor produces notable fluctuations in loading as the blades chop through concentrations of vorticity near the rotor. In fact, in the VRS, it is quite common to find evidence in the numerical calculations of local blade stall produced by locally high angles of attack. Both numerical models contain representations of the post-stall aerodynamic behaviour of the blade sections – the FVM through lookup tables and the VTM through empirical curve fits to experimental data. Representative predictions of the spanwise load distributions on the blades are shown in Fig. 11. The bias of the blade loading towards the inboard parts of the blade with the rotor in incipient VRS is noteworthy. If the rate of descent of the rotor is further increased, eventually the local lift coefficients inboard become high enough for local stall to occur. The problem is exacerbated on blades with higher twist, since these are more highly loaded inboard. The redistribution of blade lift following inboard stall affects the inflow through the rotor, the tip vortex strengths and the helical pitch of the wake structure, and can affect the mechanism of wake breakdown and the eventual onset of the VRS.

As previously described, the VRS is associated with a roughly toroidal accumulation of vorticity in the plane of the rotor. The strength of this accumulation induces high localized velocities on the blades. Figure 12 shows the spanwise load distribution on the blades for a situation where the rotor is operated deeply into the VRS. In this case, the accumulated vorticity lies in the plane of the rotor and is centred over the outer part of the disk. The high induced velocities associated with the accumulated vorticity cause negative lift production on the inboard sections of the blades, and there is no evidence of blade stall. However, the net rotor thrust under these conditions is significantly reduced when compared to the incipient VRS condition. This effect has been noted in experiments (Ref. 7).

Figure 13 shows the standard deviation of the thrust time-history for the same flight conditions that were used to generate Fig. 4 but with the rotors now operating at

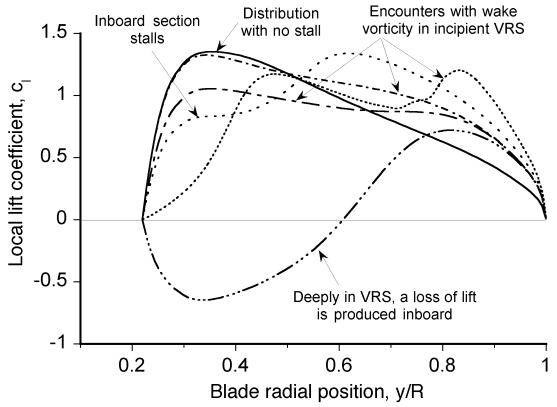

Figure 12: *Representative spanwise distributions of local lift coefficients for a rotor when deeply in the VRS condition.*

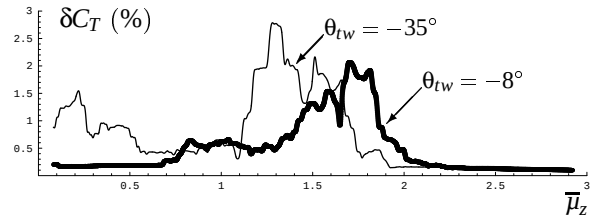

Figure 13: *Windowed standard deviation of the thrust response predicted by the FVM for an isolated rotor,* $C_T = 0.00966$*, on an accelerated* $65°$ *glideslope passing through the VRS.*

a much higher nominal thrust coefficient. For this case, the collective and cyclic pitch settings on the rotor were continually adjusted in an attempt to maintain a nominally constant thrust coefficient of 0.00966 and, again, approximately zero cyclic flapping with respect to the rotor shaft. Under these operating conditions, the rotor with the moderately twisted blades is stalled only over a small section of the inboard part of the rotor disk, while the rotor with the highly twisted blades is stalled over a much larger part of the disk. The presence of widespread stall at high descent rate has the rather counterintuitive effect of suppressing some of the effects of the VRS on the behaviour of the rotor. This is seen in Fig. 13 where at high descent rate the amplitude of the thrust perturbations experienced by the rotor with widespread stall, as a fraction of the nominal thrust coefficient of the rotor, is significantly reduced compared to the unstalled case. This reduction is partially a result of the reduced sensitivity of the rotor loads to changes in angle of attack induced by localized vorticity on those parts of the rotor blades which are operating in the post-stall regime. Similar diagrams to Figs. 7 and 8, showing snapshots of the wake structures predicted by the VTM and the FVM under these high-thrust conditions with the rotor again at a descent rate $\overline{\mu}_z = -0.8$, are shown in Figs. 14 and 15. Comparison of the vorticity maps and wake boundary plots for the rotor with the moderately-twisted blades shows differences in detail but not in the overall topology of the wake at the two different rotor thrusts. The fidelity inherent in the VTM suggests though that the loss of the lift-bearing capacity of the rotor in its stalled condition has significantly disrupted the accumulation of vorticity in the plane of the rotor compared to that seen at the lower rotor thrust coefficient. The associated decline in the excitation of the rotor from this source may also contribute to the observed reduction in amplitude of the thrust fluctuations experienced by the deeply stalled rotor. An alternative explanation may be that the loss of lift inboard simply allows the flow to propagate upward through the disk and this change in overall flow pattern may act to reduce the fluctuations in outboard portions of the wake.

Experimental Evidence

The results presented in the previous section suggest that a deeper examination of experimental VRS results might yield evidence of the influence of blade stall on the behaviour of rotors in the VRS. Both Azuma & Obata (Ref. 28) and Yaggy & Mort (Ref. 13) have reported measurements on rotors and proprotors descending into the VRS that are sufficiently detailed for this purpose. Azuma tested a small-scale helicopter rotor with a blade twist of $8°$, while Yaggy & Mort tested two proprotors with effective blade twists of $22°$ and $35°$. The two proprotors were geometrically similar, except that the rotor with $22°$

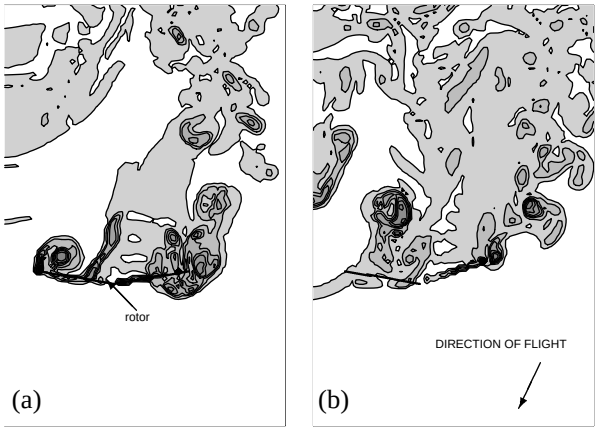

Figure 14: *Vorticity distributions in a longitudinal plane surrounding the rotor as predicted by the VTM in descending flight when* $\overline{\mu}_z = -0.8$ *and* $C_T = 0.00966$*: (a)* $\theta_{tw} = -8°$*, (b)* $\theta_{tw} = -35°$.

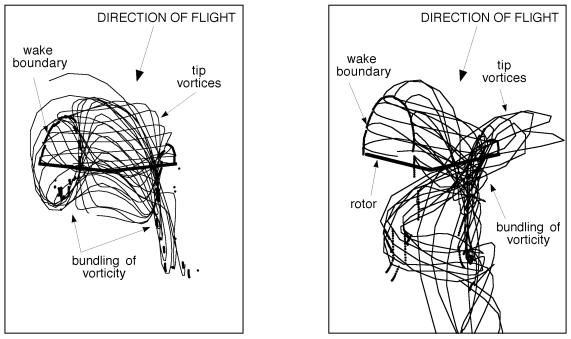

Figure 15: *Side view of wake geometry and intersections of vortex filaments in a longitudinal plane as predicted by the FVM in descending flight when* $\overline{\mu}_z = -0.8$ *and* $C_T = 0.00966$*: (a)* $\theta_{tw} = -8°$*, (b)* $\theta_{tw} = -35°$.

of blade twist had a larger root cut out and incorporated flapping hinges. In Yaggy & Mort's tests, a large range of disk loadings was covered, although, unlike in Azuma's tests, no rates of descent high enough to bring the rotors into the windmill brake state (WBS) were tested. Their data shows the expected dependence of the amplitude of the unsteady airloads on rate of descent, but also a marked dependence on blade twist and disk loading. Of course, for a particular rotor, disk loading and blade loading are proportional, and the observed sudden change in rotor behaviour with disk loading thus suggests that the published data might indeed contain evidence of the effects of blade stall on the behaviour of the rotor in the VRS.

A re-analysis of the published results for axial descending flight is shown in Fig. 16. In each case the measured amplitude of the rotor thrust fluctuations observed in the various tests is plotted as a function of the scaled rate of descent $\overline{\mu}_z$. At low rates of descent, Yaggy & Mort's data essentially collapse, using this form of scaling, to a single curve for all values of disk loading. If the thrust fluctuations are indeed produced by blade interactions with the vorticity concentrations found near the rotor disk in the VRS, then the amplitude of the fluctuations would be related to the mean bound circulation on the blades, and so to the mean rotor thrust. Some collapse of the data at low rates of descent is, therefore, to be expected. The situation is much less clear from Azuma & Obata's results because there is insufficient data to allow interpolation to constant values of disk loading. Indeed, most of the VRS data in the literature has been based on model rotor tests at fixed collective pitch, making it difficult to isolate the effects of blade loading on the rotor aerodynamics in the VRS.

For intermediate rates of descent within the VRS, Fig. 16 shows that the amplitude of the thrust fluctuations reaches a plateau before dropping off again at higher descent rates as the rotor enters the less-violent turbulent wake state (TWS) and, ultimately, the windmill brake state (WBS). The peak amplitude of the unsteady thrust fluctuations usually lies close to the conditions where the rate of descent is equal to the induced velocity through the rotor. At the lowest disk loadings, however, the regime of high thrust fluctuations extends into the region where the well-behaved flow of the WBS would usually be expected. Most interestingly, the rotor with 35° of blade twist shows much larger thrust fluctuations than the proprotor with 22° of blade twist. Both of these rotors show thrust fluctuations that are well in excess of those measured by Azuma & Obata using the rotor with only 8° of blade twist. Yaggy & Mort's data thus suggest that high blade twist, when coupled with low disk loading, produces a more violent and widespread vortex ring regime than would be associated with more moderately twisted blades. The significant dependence of these observations on disk loading implicates blade stall in the observed behaviour of the rotors. These observations are also consistent with the somewhat counterintuitive results, presented earlier, of simulations where the appearance of blade stall on the inboard parts of the rotor with highly-twisted blades at high thrust was shown to reduce the violence of the VRS.

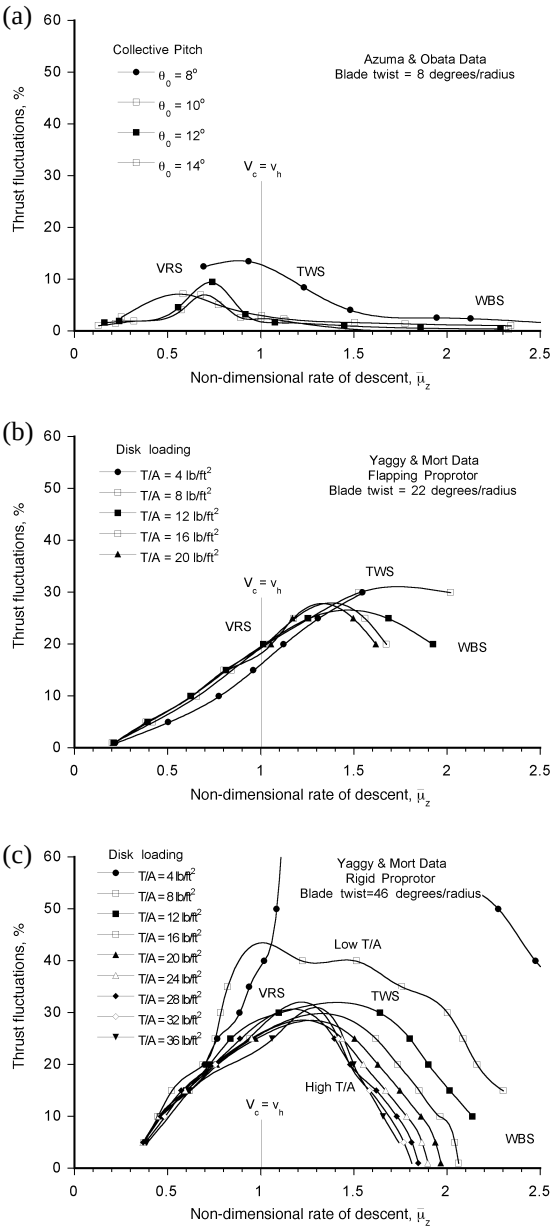

Figure 16: *Unsteady thrust fluctuations on rotors in axial descending flight through the VRS. (a) Azuma & Obata data for rotor with* $\theta_{tw} = -8°$*, (b) Yaggy & Mort data for proprotor with flapping hinges and* $\theta_{tw} = -22°$*, (c) Yaggy & Mort data for rigid proprotor with* $\theta_{tw} = -35°$.

Conclusions

A study has been conducted to examine the factors that determine the onset and development of the vortex ring state (VRS). The onset of the VRS has been shown to be related to the unstable growth of disturbances in the structure of the rotor wake. The VRS is encountered when the net convection of these growing disturbances away from the rotor becomes low enough for vorticity to accumulate near the plane of the rotor, significantly affecting blade loads and rotor performance. It has been shown that the onset of VRS, as well as the behaviour of the rotor within the

VRS, is not solely determined by the operating conditions of the rotor, such as descent rate and forward speed, but is also dependent on details of the design of the rotor such as the degree of twist incorporated into the blades. The work presented here suggests that blade stall also plays an important role in governing the behaviour of the rotor in the VRS. Numerical predictions of the onset boundary of the VRS were found generally to be in good agreement with the boundary estimated from experiments with single-rotor helicopters.

References

[1]Drees, J. M., and Hendal, W. P., "The Field of Flow Through a Helicopter Rotor Obtained from Wind Tunnel Smoke Tests," Versl. Nat. Luchtvaart Lab., Report A.1205, Feb. 1950. Also, *Journal of Aircraft Engineering*, Vol. 23, No. 266, pp. 107–111.

[2]Varnes, D. J., Duren, R. W., and Wood, E. R., "An Onboard Warning System to Prevent Hazarous Vortex Ring State Encounters," Proceedings of the 26th European Rotorcraft Forum, The Hague, The Netherlands, Sept. 26–29, 2000.

[3]Newman, S. J., Brown, R., Perry, F. J., Lewis, S., Orchard, M., and Modha, A., "Comparative Numerical and Experimental Investigations of the Vortex Ring Phenomenon in Rotorcraft," Proceedings of the 57th Annual Forum of the American Helicopter Society, Washington DC, May 9–11, 2001.

[4]Newman, S. J., Brown, R., Perry, F. J., Lewis, S., Orchard, M., and Modha, A., "Predicting the Onset of Wake Breakdown for Rotors in Descending Flight," *Journal of the American Helicopter Society*, To appear in 2002.

[5]Leishman, J. G., Bhagwat, M. J., Ananthan, S., "The Vortex Ring State as a Spatially and Temporally Developing Wake Instability," Proceedings of the American Helicopter Society International Specialists Meeting on Aerodynamics, Acoustics and Test & Evaluation, San Francisco, CA, Jan. 23–25, 2002.

[6]Leishman, J. G., Bhagwat, M. J., Ananthan, S. "Free-Vortex Wake Predictions of the Vortex Ring State for Single-Rotor and Multi-Rotor Confi gurations," Proceedings of the 58th Annual Forum of the American Helicopter Society, Montreal, June 11–14, 2002.

[7]Betzina, M. D., "Tiltrotor Descent Aerodynamics: A Small-Scale Experimental Investigation of Vortex Ring State," Proceedings of the 57th Annual Forum of the American Helicopter Society, Washington, DC, May 9–11, 2001.

[8]Scheiman, J., "A Tabulation of Helicopter Rotor-Blade Differential Pressures, Stresses, and Motions Measured in Flight," NASA TM X-952, March 1964.

[9]Brotherhood, P., "Flow Through the Helicopter Rotor in Vertical Descent," ARC R&M 2735, July 1949.

[10]Stewart, W., "Helicopter Behaviour in Vortex Ring Conditions," ARC R&M 3117, Nov. 1951.

[11]Castles, Jr., W., and Gray, R. B., "Empirical Relation between Induced Velocity, Thrust, and Rate of Descent of a Helicopter Rotor as Determined by Wind-Tunnel Tests on Four Model Rotors," NASA TN-2474, October 1951.

[12]Washizu, K., Azuma, A., K¯oo, J., and Oka, T., "Experiments on a Model Helicopter Rotor Operating in the Vortex Ring State," *Journal of Aircraft*, Vol. 3, No. 3, May–June 1966, pp. 225–230.

[13]Yaggy, P. F., and Mort, K. W., "Wind-Tunnel Tests of Two VTOL Propellers in Descent," NASA TN D-1766, March 1963.

[14]Bagai, A., Moedersheim, E., and Leishman, J. G., "Developments in the Visualization of Rotor Wakes using the Wide-Field Shadowgraph Method," *Journal of Flow Visualization and Image Processing*, Vol. 1, No. 3, July–Sept. 1993, pp. 211–233.

[15]Brinson, P., and Ellenrieder, T., "Experimental Investigation of Vortex Ring Condition," Proceedings of the 24th European Rotorcraft Forum, Marseilles, France, 1998.

[16]Wolkovitch, J., "Analytical Prediction of Vortex-Ring Boundaries for Helicopters in Steep Descents," *Journal of the American Helicopter Society*, Vol. 17, No. 3, 1972, pp. 13–19.

[17]Heyson, H. H., "A Momentum Analysis of Helicopters and Autogyros in Inclined Descent, with Comments on Operational Restrictions," NASA TN D-7917, October 1975.

[18]Peters, D. A., and Chen, S-Y., "Momentum Theory, Dynamic Infbw, and the Vortex-Ring State," *Journal of the American Helicopter Society*, Vol. 27, No. 3, July 1982, pp. 18–24.

[19]Leishman, J. G., *Principles of Helicopter Aerodynamics*, Cambridge University Press, New York, 2000.

[20]Bhagwat, M. J., and Leishman, J. G., "Stability Analysis of Rotor Wakes in Axial Flight," *Journal of the American Helicopter Society*, Vol. 45, No. 3, 2000, pp. 165–178.

[21]Bagai, A., and Leishman, J. G., "Rotor Free-Wake Modeling Using a Relaxation Technique – Including Comparisons with Experimental Data," *Journal of the American Helicopter Society*, Vol. 40, No. 3, July 1995, pp. 29–41.

[22]Bagai, A., and Leishman, J. G., "Rotor Free-Wake Modeling using a Psuedoimplicit Relaxation Algorithm," *Journal of Aircraft*, Vol. 32, No. 6, Nov.–Dec. 1995, pp. 1276–1285.

[23]Brown, R. E., "Rotor Wake Modeling for Flight Dynamic Simulation of Helicopters," *AIAA Journal*, Vol. 38, No. 1, 2000, pp. 57–63.

[24]Schumann, U., and Sweet, R. A., "A Direct Method for the Solution of Poisson's Equation with Neumann Boundary Conditions on a Staggered Grid of Arbitrary Size," *Journal of Computational Physics*, Vol. 20, No. 2, 1976, pp. 171–182.

[25]Toro, E. F., "A Weighted Average Flux Method for Hyperbolic Conservation Laws," *Proceedings of the Royal Society of London, Series A: Mathematical and Physical Sciences*, Vol. 423, No. 1864, 1989, pp. 401–418.

[26]Bhagwat, M., and Leishman, J. G., "Stability, Consistency and Convergence of Time Marching Free-Vortex Rotor Wake Algorithms," *Journal of the American Helicopter Society*, Vol. 46, No. 1, Jan. 2001, pp. 59–71.

[27]Bhagwat, M., and Leishman, J. G., "Accuracy of Straight-Line Segmentation Applied to Curvilinear Vortex Filaments" *Journal of the American Helicopter Society*, Vol. 46, No. 2, April 2001, pp. 166–169.

[28]Azuma, A., and Obata, A., "Induced Flow Variation of the Helicopter Rotor Operating in the Vortex Ring State," *Journal of Aircraft*, Vol. 5, No. 4, July–Aug. 1968, pp. 381–386.